Cell Transplantation, Vol. 25, pp. 1833–1852, 2016

0963-6897/16 $90.00 + .00
DOI: http://dx.doi.org/10.3727/096368916X691312
E-ISSN 1555-3892
www.cognizantcommunication.com

Effects of the Post-Spinal Cord Injury Microenvironment on the Differentiation Capacity of Human Neural Stem Cells Derived From Induced Pluripotent Stem Cells

Clara López-Serrano,*[1] Abel Torres-Espín,*[1] Joaquim Hernández,* Ana B. Alvarez-Palomo,† Jordi Requena,† Xavier Gasull,‡§ Michael J. Edel,†¶#[2] and Xavier Navarro*

*Group of Neuroplasticity and Regeneration, Institute of Neurosciences, Department of Cell Biology, Physiology and Immunology, Universitat Autònoma de Barcelona, and Centro de Investigación Biomédica en Red sobre Enfermedades Neurodegenerativas (CIBERNED), Bellaterra, Spain
†Control of Pluripotency Laboratory, Department of Physiological Sciences I, Faculty of Medicine, Universitat de Barcelona, Barcelona, Spain
‡Neurophysiology Lab, Department of Physiological Sciences I, Faculty of Medicine, Universitat de Barcelona, Barcelona, Spain
§Institut d'Investigacions Biomèdiques August Pi i Sunyer (IDIBAPS), Barcelona, Spain
¶University of Sydney Medical School, Westmead Children's Hospital, Division of Pediatrics and Child Health, Westmead, Australia
#School of Anatomy, Physiology & Human Biology, and Centre for Cell Therapy and Regenerative Medicine (CCTRM), University of Western Australia, Nedlands, Australia

Spinal cord injury (SCI) causes loss of neural functions below the level of the lesion due to interruption of spinal pathways and secondary neurodegenerative processes. The transplant of neural stem cells (NSCs) is a promising approach for the repair of SCI. Reprogramming of adult somatic cells into induced pluripotent stem cells (iPSCs) is expected to provide an autologous source of iPSC-derived NSCs, avoiding the immune response as well as ethical issues. However, there is still limited information on the behavior and differentiation pattern of transplanted iPSC-derived NSCs within the damaged spinal cord. We transplanted iPSC-derived NSCs, obtained from adult human somatic cells, into rats at 0 or 7 days after SCI, and evaluated motor-evoked potentials and locomotion of the animals. We histologically analyzed engraftment, proliferation, and differentiation of the iPSC-derived NSCs and the spared tissue in the spinal cords at 7, 21, and 63 days posttransplant. Both transplanted groups showed a late decline in functional recovery compared to vehicle-injected groups. Histological analysis showed proliferation of transplanted cells within the tissue and that cells formed a mass. At the final time point, most grafted cells differentiated to neural and astroglial lineages, but not into oligodendrocytes, while some grafted cells remained undifferentiated and proliferative. The proinflammatory tissue microenviroment of the injured spinal cord induced proliferation of the grafted cells and, therefore, there are possible risks associated with iPSC-derived NSC transplantation. New approaches are needed to promote and guide cell differentiation, as well as reduce their tumorigenicity once the cells are transplanted at the lesion site.

Key words: Spinal cord injury (SCI); Cell therapy; Induced pluripotent stem cells (iPSCs); Neural stem cells (NSCs); Differentiation

Received December 1, 2015; final acceptance May 26, 2016. Online prepub date: April 5, 2016.
[1]These authors provided equal contribution to this work.
[2]For correspondence on iPSCs and iNSCs: E-mail: michaeledel@ub.edu
Address correspondence to Xavier Navarro Acebes, Departamento de Biologia Celular, Fisiologia e Immunologia, Institut de Neurociències, CIBERNED, Av Can Domenech s/n, Ed. M, Campus UAB, Universitat Autònoma de Barcelona, E01893 Bellaterra, Spain. Tel: +34-935811966; Fax: +34-935812986: E-mail: xavier.navarro@uab.cat

INTRODUCTION

Spinal cord injury (SCI) is a devastating event that results in neurological deficits due to the damage of the spinal cord tissue and the interruption of ascending and descending neural pathways. There are no clinical treatments to repair the injured spinal cord. Nonetheless, in experimental studies using animal models, cell therapy has demonstrated potential beneficial effects, including cell replacement by neural stem cell (NSC) transplantation, which has produced some degree of functional recovery[1,2]. The mechanisms of action of the grafted NSCs after SCI involve secretion of neuroprotective molecules such as neurotrophic factors[3,4], which creates a permissive environment for axon regeneration[5]. This results in remyelination of spared axons by the newly formed oligodendrocytes[6] and replacement of dead cells by integration of transplanted cells within the remaining tissue for rewiring neural networks both caudal and rostral to the injury site[7].

Despite the potential of NSC transplants to promote substantial recovery in SCI animal models, the translation of this therapy into the clinic is still a challenge. Until it was discovered that somatic cells could be used to produce induced pluripotent stem cells (iPSCs), NSCs had to be obtained from embryonic stem cells (ESCs) or fetal tissue, which involve technical, immunological, and ethical problems in the clinical setting. The possibility of obtaining human NSCs from somatic cells through iPSC generation solved many of the issues that accompanied use of embryonic or fetal tissue[8]. There have been few studies that focused on the transplantation of iPSC-derived NSCs after SCI in animal models. For instance, studies in which human iPSC (hiPSC)-derived NSCs were transplanted into the injured spinal cord of mice and common marmosets showed that the procedure was safe and the cells were able to survive, differentiate into neural lineages, integrate within the host neural circuits, and promote functional recovery[1,9]. More recently, a study in rats with SCI showed that grafted iPSC-derived NSCs were able to differentiate into cells of the three neural lineages and integrate into the central nervous system (CNS), but, contrary to the previous studies, the transplant did not lead to improvement in motor function[10].

Although iPSCs are becoming a promising source for NSC transplantation after SCI, there are still some concerns regarding their use for clinical applications, such as the potential introduction of transgenes as a result of using viral vectors, immunological rejection, and a possible greater risk of tumor formation if the somatic cells are not completely reprogrammed or remain undifferentiated[11]. These issues need to be addressed by extensive preclinical investigation.

Therefore, it is still uncertain if transplantation of iPSC-derived NSCs may be a good therapy for restoring the damaged tissue after SCI. Very recent studies have also shown controversial outcomes after iPSC-derived NSC transplantation in different animal models, from absence of functional recovery[12] to successful engraftment, differentiation, and recovery of the animals after the initial injury[13]. Thus, the aim of the present study was to characterize the differentiation pattern of the iPSC-derived NSCs once transplanted into the damaged spinal cord. We used human NSCs derived from iPSCs generated from adult fibroblasts, which present advantageous features, including the differentiation of transplanted stem cells. These cells are able to differentiate into any of the three main neural cell types and do not raise compatibility issues for application in humans as they can be obtained from adult somatic cells, allowing for autologous transplantation[14]. We transplanted rats with iPSC-derived NSCs acutely and subacutely after SCI to study how the injury environment affected survival and differentiation of the cells. We observed a detrimental effect on the functional recovery of the transplanted animals and continuous proliferation as well as noncomplete differentiation of the cells. Therefore, our findings indicate that the differentiation pattern of the engrafted cells is crucial for a successful functional recovery after SCI and that further studies are necessary.

MATERIALS AND METHODS

hiPSC and iPSC-Derived NSC Culture

The procedure for genetic manipulation and generation of iPSCs from human fibroblasts was reviewed and approved by the Ethical Committee of the University of Barcelona. Adult human dermal fibroblasts from a healthy 48-year-old male volunteer donor, who signed a written informed consent form, were subjected to retroviral transduction[15] with plasmids encoding for the vesicular stomatitis virus glycoprotein (VSV-G) and the reprogramming factors octamer-binding transcription factor 3/4 (OCT 3/4), (sex determining region Y)-box 2 (SOX2), Kruppel-like factor 4 (KLF4), and C-MYC, and the cells were split into six-well plates (Gibco, Thermo Fisher Scientific, Grand Island, NY, USA). After 3–4 weeks, colonies were then picked and expanded to establish 18 hiPSC lines, 3 of which were characterized for pluripotency markers, morphology, transgene silencing, and differentiation. Then the hiPSCs were adapted to feeder-free culture conditions on Matrigel (Thermo Fisher Scientific, Waltham, MA, USA)-coated plates using Essential 8 feeder-free medium (Thermo Fisher Scientific). After 1 day of splitting, hiPSCs were induced to iPSC-derived NSCs according to Life Technologies (now Thermo Fisher Scientific) protocols (www.thermofisher.com) and using Gibco iPSC Neural Induction Medium (Gibco, Thermo Fisher Scientific) for 7 days. Passage 0 (P0) iPSC-derived NSCs were then ready for

cryopreservation, expansion, or differentiation. Cryopreserved P0 iPSC-derived NSCs were recovered from 1-ml vials and plated in Geltrex matrix-coated vessels (Gibco). The cells were suspended within complete Neural Expansion Medium (Gibco) to a concentration of 2×10^5 cells/ml. Rho-associated coiled-coil kinase (ROCK) inhibitor Y27632 (Sigma-Aldrich, St. Louis, MO, USA) at a final concentration of 5 μM was added to the cell suspension to prevent cell death. After overnight incubation, medium was changed to complete Neural Expansion Medium to eliminate the ROCK inhibitor Y27632. Neural Expansion Medium without Y27632 was changed every 2 days.

Electrophysiological In Vitro Study of iPSC-Derived NSCs

Standard patch clamp electrophysiological recordings were performed with an Axopatch 200B amplifier (Molecular Devices, Sunnyvale, CA, USA) on differentiated iPSCs grown on glass coverslips. Membrane currents were recorded in the whole-cell configuration with a holding voltage of −60 mV, filtered at 2 kHz, digitized at 10 kHz, and acquired with pClamp 9 software (Molecular Devices). Voltage pulses (400 ms) were applied from −100 to +50 mV in 10-mV increments to record sodium and potassium voltage-activated currents. Cells were placed in a physiological bath solution: 145 mM NaCl, 5 mM KCl, 2 mM $CaCl_2$, 2 mM $MgCl_2$, 10 mM HEPES (Sigma-Aldrich) at pH 7.4. Electrodes had a resistance between 2 and 4 MΩ when filled with intracellular solution: 140 mM KCl, 2.1 mM $CaCl_2$, 2.5 mM $MgCl_2$, 5 mM ethylene glycol tetraacetic acid (EGTA) (Sigma-Aldrich), 10 mM HEPES at pH 7.3. All recordings were done at room temperature (RT; 22–23°C). Tetrodotoxin (TTX; 2 μM) (Alomone Labs, Jerusalem, Israel) was used to block sodium currents as indicated in Figure 1G. Sodium currents were measured at the peak inward current. Potassium currents were measured at the end of the voltage pulse.

Assay of iPSC-Derived NSC Viability in Cultures Exposed to Spinal Cord Lysate

The viability of the cells in culture was assessed under the influence of spinal cord lysate, obtained from either noninjured rats or rats subjected to spinal cord contusion 7 or 14 days earlier, as explained below. Rats were sacrificed, and a spinal cord segment 1 cm long centered at the epicenter of the injury (or equivalent segment in intact animals) was immediately removed, resuspended in Dulbecco's modified Eagle's medium (DMEM) (Thermo Fisher Scientific), and sonicated for 20 s with an Ultrasonic Homogenizer 300 (BioLogics, Grenoble, France) to obtain lysate. Quantification of the protein content was done by the bicinchoninic acid (BCA) method (Pierce BCA Protein Assay Kit; Thermo Fisher Scientific), and 50 μg protein/ml of lysate was used in the experiments.

Cell viability was determined by the tetrazolium salt 3-[4,5-dimethylthiazol-2-yl]-2,5-diphenyltetrazolium bromide assay (MTT; Sigma-Aldrich). iPSC-derived NSCs (from the same batch as the ones used in the transplantation experiment, see below) were plated in 96-well culture plates (Thermo Fisher Scientific) at a density of 2×10^5 cells/ml with Neural Expansion Medium containing the supernatant from the injured spinal cord lysate at a concentration of 50 μg/ml for 1 to 3 days. Then 10 μl of MTT solution (4 mg/ml) was added to each well at a final concentration of 0.2 mg/ml. Cells were incubated at 37°C for 2 h. After incubation, the medium was aspirated, and 200 μl of dimethyl sulfoxide (DMSO; Sigma-Aldrich) was added. The absorbance value was measured in a multiwell spectrophotometer (Bio-Tek, Winooski, VT, USA) at 490 and 620 nm.

Spinal Cord Injury

Adult female Sprague–Dawley (SD) rats (9 weeks old, 250–300 g) were provided by the animal facility of the Universitat Autònoma de Barcelona. The animals were housed with free access to food and water at RT (22 ± 2°C). The experimental procedures were approved by the Ethical Committee on Animal Experimentation of the Universitat Autònoma de Barcelona and were in accordance with the European Communities Council Directive (2010/63/EU).

Operations were performed under ketamine (Imalgene 1000; Merial, Santiago, Chile) and xylazine (Rompun; Bayer DVM, Shawnee Mission, KS, USA) anesthesia [90/10 mg/kg administered via intraperitoneal (IP) injection]. A longitudinal dorsal incision was made to expose T6–T10 spinous processes. A laminectomy was performed in T8–T9 vertebra, and a cord contusion of 200 kdyn was induced using an Infinite Horizon Impactor (Precision Systems and Instrumentation, Lexington, KY, USA). A set of six rats were injured to obtain the spinal cord lysate for the culture experiment (see above). For the transplantation, experimental animals were divided into three groups. One group of rats was transplanted acutely, at 0 days postinjury (dpi) with iPSC-derived NSCs ($n = 12$). The other two groups of rats were transplanted subacutely, at 7 dpi, with vehicle [phosphate-buffered saline (PBS); Sigma-Aldrich] ($n = 6$) and with iPSC-derived NSCs ($n = 12$). Cells that were to be transplanted were suspended in PBS at a concentration of 75,000 cells/μl and kept on ice during the time of the surgery. The cell viability at the time of injection was around 90% as quantified in a Neubauer chamber (Brand, Wertheim, Germany) with trypan blue stain (Sigma-Aldrich). Using a glass needle (100-μm internal diameter; Eppendorf,

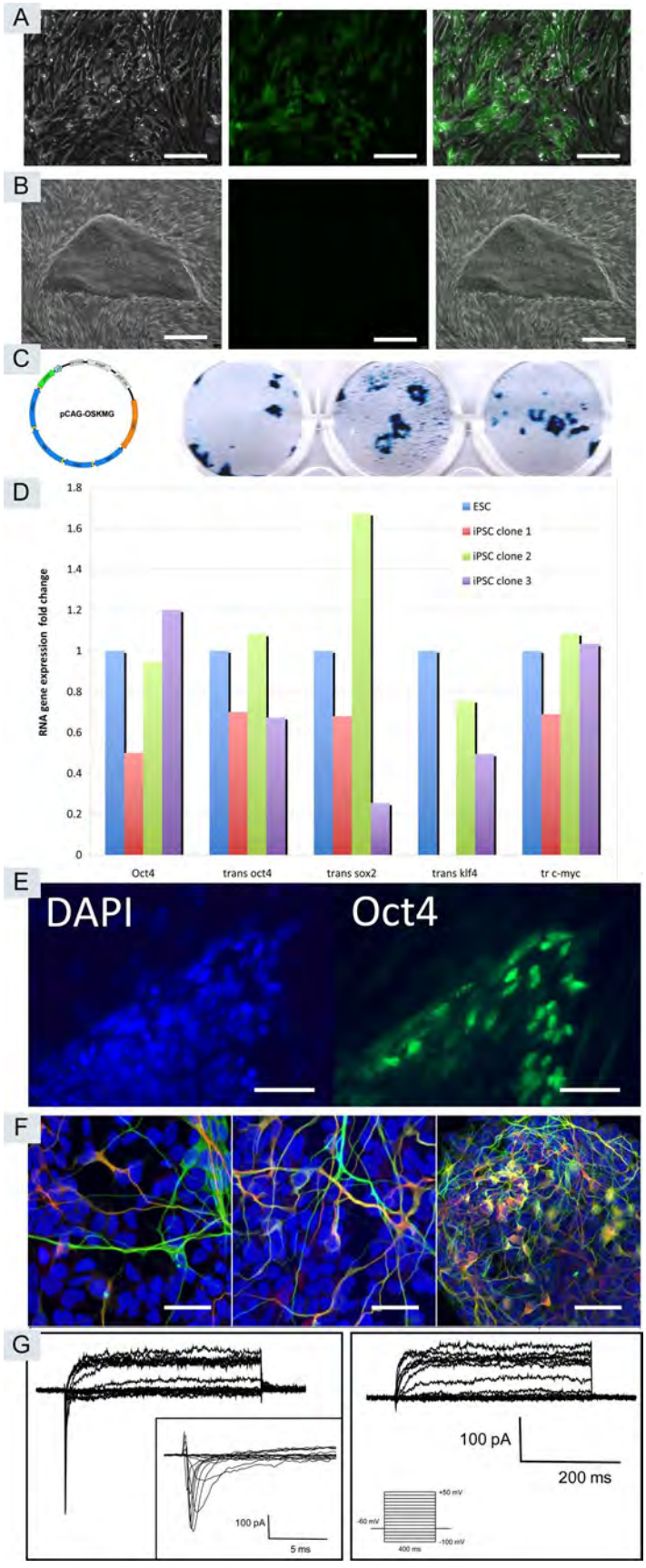
A
B
C
pCAG-OSKMG
D
RNA gene expression fold change
1.8
1.6
1.4
1.2
1
0.8
0.6
0.4
0.2
0
ESC
iPSC clone 1
iPSC clone 2
iPSC clone 3
Oct4
trans oct4
trans sox2
trans klf4
tr c-myc
E
DAPI
Oct4
F
G
100 pA
5 ms
100 pA
200 ms
+50 mV
-60 mV
-100 mV
400 ms

Hamburg, Germany) coupled to a 10-µl Hamilton syringe (Hamilton #701; Hamilton Co., Reno, NV, USA), 6 µl of the cell suspension or vehicle (PBS) was intraspinally injected at the injury epicenter, and 4 µl was injected 2 mm rostral and caudal to the injured center, for a total of 1×10^6 cells per rat. A perfusion speed of 2 µl/min was controlled by an automatic injector (KDS 310 Plus; KD Scientific, Holliston, MA, USA), and the needle tip was maintained inside the tissue for 3 min after each injection to avoid reflux. The wound was sutured and the animals were allowed to recover in a warm environment. Postoperative analgesia was provided with buprenorphine (0.05 mg/kg; RB Pharmaceuticals, Berkshire, UK).

In order to prevent immune rejection of the xenogeneic grafted cells, immunosuppression was provided. A subcutaneous injection of FK506 (Fujisawa Pharmaceuticals, Osaka, Japan) was administered immediately after the transplantation (2 mg/kg), and additional injections of FK506 (1 mg/kg) were given once a day until the end of the follow-up to all rats in each experimental group. Bladders were expressed twice a day until reflex voiding of the bladder was reestablished. To prevent infection, amoxicillin (500 mg/L; Laboratorios Normon, Madrid, Spain) was given in the drinking water for 1 week.

Functional Assessment

Open-Field Locomotion. Motor behavior was tested after surgery once a week until 63 days posttransplant (dpt). Animals were placed individually in an open field and allowed to move freely for 5 min. Two observers evaluated locomotion during open-field walking and scored the hindlimb performance, according to the Basso, Beattie, Bresnahan (BBB) scale[16], ranging from 0 (no movement) to 21 (normal movement), and to the BBB subscale[17].

Treadmill Locomotion. The maximal walking speed was assessed under treadmill conditions once a week, starting 2 weeks after injury when the animals were able to walk, until 63 dpt. The treadmill speed was progressively increased from 0 cm/s until the animal was not able to run with weight support at the selected speed.

Electrophysiological Tests. The rats were anesthetized with pentobarbital (30 mg/kg by IP injection; Sigma-Aldrich), placed prone onto a metal plate, and skin temperature was maintained above 32°C. An electromyograph (Sapphire 4ME; Vickers Healthcare Co., Woking, UK) was used for the tests. Motor nerve conduction tests were performed by stimulating the sciatic nerve with single electrical pulses (100 µs at supramaximal intensity) delivered by needles inserted percutaneously at the sciatic notch, and recording the compound muscle action potentials (CMAPs) of the tibialis anterior (TA) and gastrocnemius medialis (GM) muscles by means of needle electrodes. The active electrode was inserted on the belly of the muscle and the reference at the fourth toe. The peak latency and the onset-to-peak amplitude of the maximal M waves were measured.

Motor-evoked potentials (MEPs) were elicited by transcranial electrical stimulation of the brain. Two needle electrodes were placed subcutaneously over the skull; the anode was placed over the sensorimotor cortex, and the cathode was placed on the nose. Single electrical pulses of supramaximal intensity (25 mA, 100 µs) were applied, and the MEPs were recorded with monopolar needle electrodes from the TA and GM muscles. The MEP/M amplitude ratio was calculated to provide the proportion of motor units activated by transcranial electrical stimulation relative to the total pool of spinal motoneurons.

All of the animals were used for functional assessment at different time points. However, animals needed for histological study at 7 and 21 dpt (see below) were randomly withdrawn from the study at such time points. The final numbers of animals considered at different times for functional assessment were as follows: vehicle group ($n = 6$ for all the time points), acute transplant group

FACING PAGE

Figure 1. Characterization of human induced pluripotent stem cells (hiPSCs) and differentiation into neural stem cells (NSCs) and neurons. (A) Photos of retroviral infected fibroblast cells at day 3 postinfection showing high efficiency of transduction based on the polycistronic green fluorescent protein (GFP)-tagged vector. (B) Photographs of hiPSC colony on iHFFs (inactivated human foreskin fibroblasts) feeder layer and negative GFP signal demonstrating that the transgene is silenced in the hiPSC clones. Note the good morphology of the colony with sharp defined boundaries. (C) Map of the polycistronic retroviral vector containing Oct4, Sox2, Klf4, and c-Myc in a single expression vector (GFP tagged). Left panels show pluripotency marker, alkaline phosphatase staining (blue) of 3 of the 18 iPSC clones made. (D) Reverse transcription polymerase chain reaction (RT-PCR) gene expression analysis of pluripotency marker Oct4 in three hiPSC clones using human embryonic stem cells (hESCs) as a positive control (normalized to 1). All three hiPSCs express high levels of Oct4. Transgene expression of Oct4, Sox2, Klf4, and c-Myc was also analyzed to confirm negative GFP signal for all four factors confirming that the transgene is switched off in hiPSC clones. (E) Immunofluorescence staining of Oct4 (green) protein expression in hiPSC colony. (F) Differentiation to NSCs and neurons. Left: After 1 week in neurobasal medium plus N2/B27 plus RA (1 mM) and stained for TUJ1 (green) and MAP2 (red) and 4′,6-diamidino-2-phenylindole (DAPI) (blue). Middle: After 10 days of differentiation to neurons. Right: After 4 weeks, note that a complex neural network of TUJ1/MAP2-positive neurons has formed. (G) Patch clamp analysis. Left: Representative traces of voltage-activated Na^+ and K^+ currents in iPSC-derived neurons recorded with the whole-cell configuration of the patch clamp technique. Cells were held at −60 mV, and voltage pulses were applied from −100 to +50 mV to activate the currents. Inset: Magnification of the voltage-activated Na^+ currents recorded. Right: Application of 2 µM tetrodotoxin significantly blocked inward Na^+ currents in the recording shown at left but did not affect outward K^+ currents. Scale bars: 200 µm (A, B), 100 µm (E, F).

($n=12$ from 0 to 7 dpi, $n=8$ at 14 and 21 dpi, and $n=5$ until the end of the follow-up), and subacute transplant group ($n=12$ from 0 to 14 dpi, $n=9$ at 21 and 35 dpi, and $n=6$ until the end of the follow-up).

Tissue Processing and Immunohistochemical and Histological Analyses

For cell tracking, rats from both acute and subacute transplantation groups were sacrificed at 7 ($n=3$ for each group), 21 ($n=4$ for acute and $n=3$ for subacute group), and 63 days ($n=5$ for acute and $n=6$ for subacute group) after transplantation. Rats were deeply anesthetized (pentobarbital, 100 mg/kg IP) and intracardially perfused with 4% paraformaldehyde (PFA; Sigma-Aldrich) in PBS. The spinal cord segment from 1 cm rostral to 1 cm caudal of the injury epicenter (2 cm total length) was harvested and postfixed in the same fixative solution for 4 h and cryopreserved in 30% sucrose. Before sectioning, macrograph pictures of the spinal cord segment were obtained under the microscope. For evaluation of the spared tissue, grafted area, and cell differentiation, transverse spinal cord sections (30 μm thick) were cut with a cryotome (Leica CM190; Leica Microsystems, Wetzlar, Germany) and distributed in 12 series of 24 sections (separated by 360 μm) each. Sections were collected onto gelatin-coated glass slides.

Spinal cord sections and cell cultures were processed for immunohistochemistry (IHC) and immunocytochemistry (ICQ) with specific antibodies for human stem cells, including SC121 against cytoplasm protein (1:100; Stem Cells Inc., Newark, CA, USA) and SC101 against nuclear protein (1:500; Stem Cells Inc.) to localize the engrafted cells. Other transverse sections, as well as iPSC-derived NSC cultures, were immunostained with a primary antibody against glial fibrillary acidic protein (GFAP; 1:100; Dako, Glostrup, Denmark; GFAP, 1:500; Sigma-Aldrich) to visualize astroglial reactivity and the glial scar around the lesion. To characterize the iPSC-derived NSC phenotype after transplantation, we used antibodies against NeuN (1:1,000; LifeSpan BioSciences, Seattle, WA, USA) and β-III tubulin (1:500; BioLegend, San Diego, CA, USA) to label neurons, 2′,3′-cyclic-nucleotide 3′-phosphodiesterase (CNPase; 1:100; Merck-Millipore, Darmstadt, Germany) and Ng2 (1:500; Merck-Millipore) for oligodendrocytes, Ki-67 (1:100; Abcam, Cambridge, UK) for cells in proliferation, and nestin (1:500; Covance) to identify iPSC-derived NSCs in a nondifferentiated state. To label immune cells recruited around the transplant, we used anti-Iba1 (1:1,000; Wako, Richmond, VA, USA) (primary antibodies used are summarized in supplementary Table 1, available at https://www.dropbox.com/sh/aiaq83057uij1c0/AADTehQ_p4b524GALv1H14Zya?dl=0). Tissue sections were blocked with PBS supplemented with 0.3% Triton (Sigma-Aldrich) and 5% species-specific serum and incubated for 24 h at 4°C with the corresponding primary antibody diluted in PBS plus 0.3% Triton and 2.5% fetal bovine serum (FBS; Sigma-Aldrich). After washes, sections were incubated for 2 h at RT with secondary antibody (donkey anti-mouse Alexa Fluor 488 for SC121, SC101, and GFAP; donkey anti-rabbit Alexa Fluor 594 for GFAP, β-III tubulin, Ki-67, Ng2, and nestin; and goat anti-chicken Alexa Fluor 594 for NeuN and CNPase; all at 1:200; Thermo Fisher Scientific) in conjunction with 4′,6-diamidino-2-phenylindole (DAPI; 1:10,000; Invitrogen, Thermo Fisher Scientific, Carlsbad, CA, USA). Slides were dehydrated and mounted with Citoseal 60 (Thermo Fisher Scientific). In all IHC procedures, we included internal controls (for primary and secondary antibodies) to detect nonspecific staining.

Table 1. Antibodies Used for Immunolabeling in This Study

Antibody	Description	Cell Target	Host Species	Dilution	Company
NeuN	Neuron-specific nuclear protein	Mature neurons	Chicken	1:1,000	LifeSpan BioSciences
β-III tubulin	Neural microtubule element	Immature neurons	Rabbit	1:500	Covance
GFAP	Glial fibrilary acidic protein	Glial cells	Rabbit Mouse	1:100 1:500	Dako Cytomation Sigma
CNPase	Constituent of cells that elaborate myelin	Mature oligodendrocytes	Chicken	1:100	Millipore
Ng2	Proteoglycan of oligodendroglial precursors	Immature oligodendrocytes	Rabbit	1:500	Millipore
Ki-67	Present during G_1, S, G_2, and M phases	Proliferative cells	Rabbit	1:100	Abcam
Nestin	Intermediate filament	Neural progenitor cells	Rabbit	1:500	Covance
SC101	Present in human nuclei	Human cells	Mouse	1:500	Stem Cells
SC121	Present in human cytoplasm	Human cells	Mouse	1:100	Stem Cells
Iba1	Calcium binding protein	Microglia/macrophages	Rabbit	1:1,000	Wako

Images were obtained with a digital camera (Olympus DP50; Olympus, Münster, Germany) attached to a microscope (Olympus BX51). Analysis of spared tissue and graft area was made using 36 transversal cord sections (separated by 360 μm) of each animal. Consecutive images of the SCI segments were taken at 4× with the same settings. The areas of spared tissue, of the cavity, and of the total spinal cord section were delineated and measured using ImageJ software [National Institutes of Health (NIH), Bethesda MA, USA]. Volume of spared tissue was calculated using the Cavalieri's correction of morphometric volume[18]. A spinal cord segment three-dimensional reconstruction representative of each group was made using the Reconstruct software (http://synapses.clm.utexas.edu/software-0)[19]. Analysis of colocalization of the different markers was made in transverse cord sections of each animal. Images of the SCI segments were taken at 10× with a confocal laser microscope by using Zen Software (ZEISS LSM 700; Zeiss, Jena, Germany). The area of colocalization was measured using the ImageJ software.

Statistical Analysis

Quantitative data of functional and morphological studies were analyzed by repeated-measures two-way analysis of variance (ANOVA). Bonferroni's post hoc test was used for comparing pairs of groups. In all the comparisons, $p<0.05$ was considered as significant and data are presented as mean ± standard error of the mean (SEM). Statistical analyses were performed with Prism 7 software (GraphPad, La Jolla, CA, USA).

RESULTS

In Vitro Characterization of hiPSC and iPSC-Derived NSC Phenotype

hiPSCs were characterized in vitro for pluripotency markers, morphology, transgene silencing, and differentiation into neurons (Fig. 1). Retroviral infection of the four pluripotency genes into human foreskin fibroblasts (HFFs) was performed with very high efficiency (70%), and emerging iPSC colonies had a perfect morphology with well-defined borders and were negative for transgene activation based on green fluorescent protein (GFP) signal after two to three passages (Fig. 1A and B). All colonies expressed pluripotency markers for alkaline phosphatase and high Oct4 gene expression (Fig. 1C–E). Analysis of transgene expression of all four reprogramming factors by reverse transcription polymerase chain reaction (RT-PCR) confirmed the negative GFP signal that all transgene expressions had been silenced in the hiPSC clones. The iPSCs were able to differentiate into ectoderm with high efficiency based on TUJ1/MAP2 protein markers by immunofluorescence analysis (Fig. 1F). The iPSCs were also able to differentiate into endoderm and mesoderm (data not shown).

iPSC-derived neurons recorded in patch clamp studies presented small inward currents with activation and deactivation properties characteristic of voltage-gated Na^+ currents (Fig. 1G). Na^+ currents started activating at −30 mV, and mean peak current amplitude was −176.5 ± 81.1 pA ($n=4$). Bath application of 2 μM TTX produced an 80–90% block of the currents, thus assuring that these were produced by activation of voltage-gated Na^+ channels. Outward potassium currents were also seen in all cells recorded, with a mean current of 52.8 ± 9.2 pA ($n=4$). The currents recorded from iPSC-derived neurons were of small amplitude compared with primary neurons, but they presented the typical characteristics of Na^+ and K^+ voltage-activated currents in neurons. Small amplitudes probably indicate a still low expression of these channels at this cell differentiation stage.

Effects of iPSC-Derived NSC Transplantation on Functional Recovery After SCI

Open-Field Locomotion. The BBB open-field locomotion score was used to test gross voluntary locomotion after SCI. All of the injured rats showed complete paralysis of the hind limbs (0 score) at 3 dpi, followed by partial recovery during the following 2 weeks. The animals achieved a plateau without significant further recovery during the next 5 weeks with a BBB score of about 10–11 points, indicating weight support and occasional/frequent plantar stepping performance. During the early phase, there were only mild differences between the group acutely transplanted and the other groups. At 63 dpt, both acutely and subacutely cell-transplanted groups showed a slight, although not significant, decrease in the BBB score compared to the vehicle group (acute transplant group: 9.83 ± 0.25; subacute transplant group: 9 ± 0.14; and vehicle: 10.71 ± 0.34) (Fig. 2A). In the BBB subscale (from 0 to 13), which measures fine walking ability, both cell-transplanted groups had progressively lower scores than the vehicle group during the last 5 weeks of the follow-up (at 63 dpt, acute transplant group: 0.25 ± 0.17; subacute transplant group: 0 ± 0; and vehicle: 1.91 ± 0.96), with significant differences between the vehicle and the subacute groups (Fig. 2B).

Treadmill Locomotion. Noninjured animals were able to run at a maximum treadmill speed of 80 cm/s. In all SCI groups, the rats did not support their weight in stance and none were able to run during the first 2 weeks after surgery. The acute transplant rats showed a lower speed than the subacute group around the 4th week of follow-up (at 28 dpt, acute transplant group: 21.1 ± 3.14 cm/s; subacute transplant group: 25.2 ± 6.37 cm/s; vehicle: 27.5 ± 6 cm/s). At later time points there was a decrease in the maximal treadmill speed in both treated groups (at 63 dpt, acute transplant group: 13.3 ± 3.8 cm/s; subacute

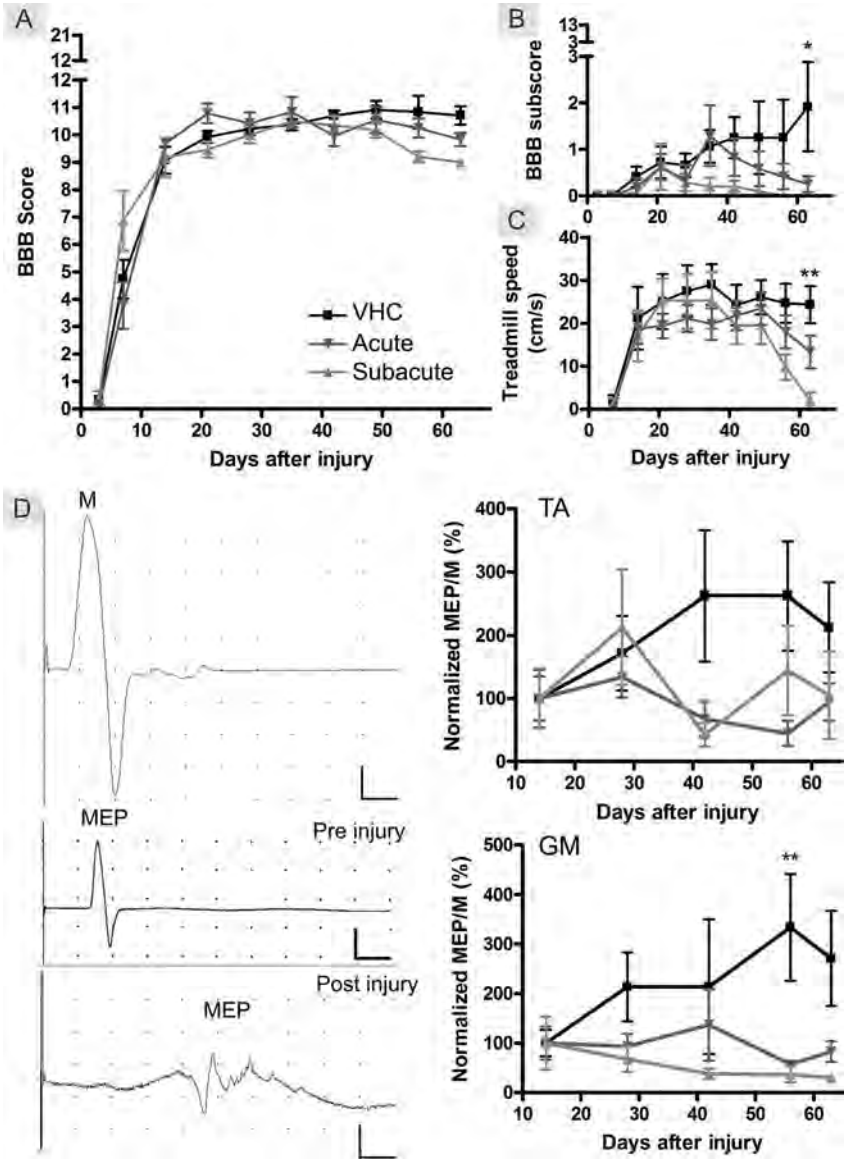

Figure 2. Effect of iPSC-derived NSC grafts on functional recovery after spinal cord injury (SCI). Open-field locomotion was evaluated weekly after SCI using the score (A) and subscore (B) of the Basso, Beattie, Bresnahan (BBB) scale in the three studied groups. All the animals showed complete paralysis of the hindlimbs at 3 days postinjury, followed by a recovery phase reaching a BBB score between 9 and 11, and a later decrease of the score in the transplanted groups. Maximum speed that animals were able to walk supporting their weight on a treadmill was also measured every week, showing a decrease from 40 days postinjury in the transplanted rats (C). Compound muscle action potentials (CMAPs) and motor-evoked potentials (MEPs) from tibialis anterior (TA) and gastrocnemius (GM) muscles were recorded every other week starting 2 weeks after injury. The CMAP amplitude (D, top panel) did not change during the follow-up (data not shown). Contrarily, the MEP was markedly reduced in amplitude and delayed in latency after injury (D, bottom panel) in comparison with noninjured animals (D, middle panel). The ratio MEP/M, used to normalize the evolution of the MEP responses (D, graphs), showed an increase over time in nontransplanted animals and a decrease in transplanted rats during follow-up. Scales in (D) top and middle recordings: vertical bar = 2 mV, horizontal bar = 2 ms; (D) bottom recording: vertical bar = 50 μV, horizontal bar = 5 ms. *$p < 0.05$, **$p < 0.01$ vehicle (VHC) group versus acute and subacute transplanted groups.

transplant group: 2 ± 2 cm/s; vehicle: 24.3 ± 4.3 cm/s), which was more marked in the subacute group (Fig. 2C).

Motor-Evoked Potentials. The normal MEPs were abolished during the follow-up after SCI in most rats, and only a few animals presented a very small response (<50 μV in amplitude) at the normal latency. A late MEP response (latency ~20 ms) appeared after injury in TA and GM muscles with increasing amplitude in the vehicle group over time. In contrast, the late MEP responses decreased from 28 dpt until the end of the follow-up in

the cell-transplanted groups compared to the vehicle-injected group (Fig. 2D).

Taken together, the data suggest a late reduction of the functional recovery achieved during the first weeks after transplantation of iPSC-derived NSC-transplanted animals.

iPSC-Derived NSCs Survived and Proliferated in the Injured Spinal Cord, Affecting the Amount of Spared Tissue

Spinal Cords at 63 Days After Transplantation. After SCI, tissue compression occurs as shown in the spinal cord images of vehicle-treated animals. In contrast, animals from the cell-transplanted groups demonstrated an increase of the volume occupied by the grafted cells along the lesion site, which was reflected by the area of the spinal cord segment (Fig. 3A).

Spared Tissue After SCI. We then evaluated the amount of spared tissue at 63 days after transplantation in transverse cross sections of the spinal cord that were immunostained for GFAP. The amount of preserved tissue was significantly higher in areas both rostral and caudal to the epicenter in the animals who received vehicle injections (Fig. 3B and E) than in those injected with iPSC-derived NSCs (Fig. 3C and D). Despite the fact that no significant differences were observed between groups at the epicenter of the lesion, the total volume of preserved tissue was significantly smaller in the groups transplanted with the cells (Fig. 3E).

Grafted Cell Localization and Survival. We evaluated the area of spinal cord occupied by iPSC-derived NSCs at 7, 21, and 63 dpt along the injured spinal cord segment. The grafted cells were stained with the human cytoplasmic marker SC121 to identify the grafted cells. The area occupied by iPSC-derived NSCs was significantly larger at 63 dpt than at 7 and 21 dpt in both transplanted groups (Fig. 4). Detailed observation of spinal cord cross sections showed increasing cell graft volume with time in the epicenter and also caudal and rostral to the lesion (supplementary Fig. 3A–F; available at: https://www.dropbox.com/sh/aiaq83057uij1c0/AADTehQ_p4b524GALv1H14Zya?dl=0).

Immune Cell Recruitment Around iPSC-Derived NSC Transplant. We evaluated the presence of immune cells in the cell graft at 63 dpt by using an antibody against Iba1. We observed recruitment of microglia and monocytes at the edge and in the middle of the graft in both groups of transplanted animals (supplementary Fig. 4A–C; available at: https://www.dropbox.com/sh/aiaq83057uij1c0/AADTehQ_p4b524GALv1H14Zya?dl=0).

iPSC-Derived NSC Proliferation. In order to assess proliferation, we stained the transplanted cells with the human nuclear marker SC101 and the proliferation marker Ki-67 in samples taken at 7, 21, and 63 dpt (Fig. 5A). By confocal microscopy, we observed colocalization of both markers (Fig. 5B). The percentage of area occupied by Ki-67 in relation to the total area occupied by SC101 indicated that iPSC-derived NSCs in the spinal cords showed higher proliferation at 7 dpt compared to 21 and 63 dpt (Fig. 5C).

iPSC-Derived NSC Differentiation Within the Injured Spinal Cord

Phenotype of iPSC-Derived NSCs Before Transplantation. iPSC-derived NSCs were cultured in vitro and stained with a combination of differentiation markers to characterize their phenotype at passage 3, just before transplantation. Other cells from the same culture and passage were used for in vivo transplantation. Immunohistochemical analysis in vitro showed that iPSC-derived NSCs at passage 3 expressed nestin, β-III tubulin, and Ki-67, but no expression of the markers NeuN, GFAP, CNPase, and Ng2 was observed (supplementary Fig. 1A–L; available at: https://www.dropbox.com/sh/aiaq83057uij1c0/AADTehQ_p4b524GALv1H14Zya?dl=0), indicating that before grafting, the cells maintained a neural stem and proliferative phenotype.

Transplanted iPSC-Derived NSC Phenotype. Spinal cord sections from the transplanted groups were immunostained with a combination of differentiation markers. We observed that some iPSC-derived NSCs, identified by labeling with the human markers SC101 or SC121, were also positive for GFAP, Nestin, NeuN, and β-III tubulin, but no colocalization with either CNPase or Ng2 was observed (supplementary Fig. 2A–F; available at: https://www.dropbox.com/sh/aiaq83057uij1c0/AADTehQ_p4b524GALv1H14Zya?dl=0). We then measured the percentage of colocalized area of these markers in spinal cord sections at 7, 21, and 63 dpt in both transplanted groups. Regarding the expression of the neural marker β-III tubulin (Fig. 6), the percentage of colocalized area with SC121 increased significantly from 7 dpt (acute iPSC-derived NSC transplant group: 71.31 ± 2.30%; subacute iPSC-derived NSC transplant group: 59.9 ± 2.05%) to 63 dpt (acute transplant group: 85.60 ± 2.75%; subacute transplant group: 88.08 ± 1.78%) in both transplanted groups. Similarly, the colocalized area of the neural marker NeuN with the human marker SC101 was significantly higher at 63 dpt (acute transplant group: 15.70 ± 9%; subacute transplant group: 30.55 ± 10%) than at 7 (acute transplant group: 3.17 ± 3%; subacute transplant group: 0.30 ± 0%) or 21 dpt (acute transplant group: 5.13 ± 2%; subacute transplant group: 6.95 ± 2%) in both groups (Fig. 6A–D). Regarding glial phenotype markers, measurements of iPSC-derived NSCs expressing the astroglial marker GFAP showed differences between the center and the edge of the graft (Fig. 7). In the middle of the graft, we observed a slight increase of cells from 7 (acute transplant

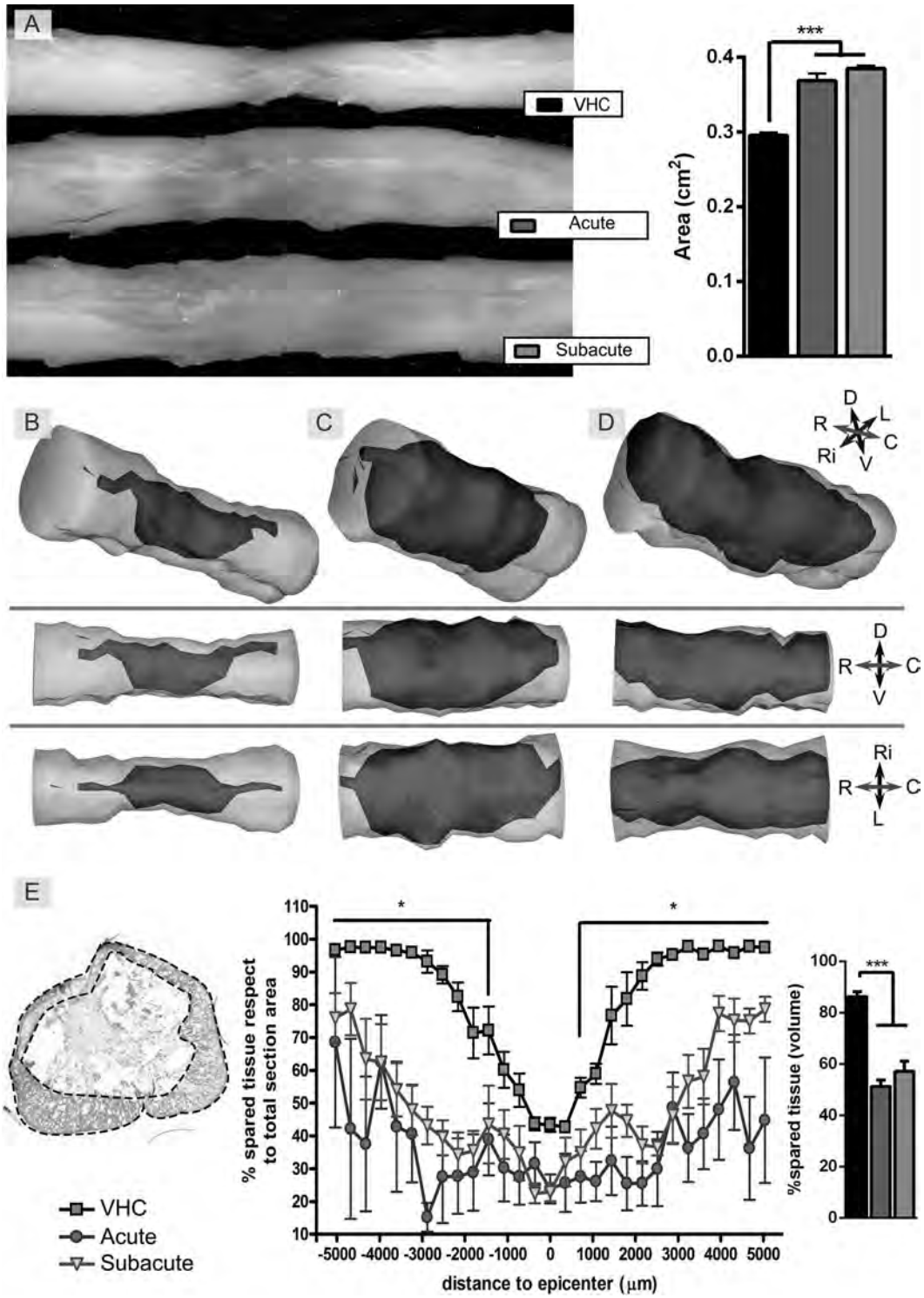

Figure 3. The spared tissue at the end of the follow-up was reduced by the cell graft. Representative photographs of spinal cords at 63 days after cell grafting showing an enlargement at the injury site in the iPSC-derived NSC-transplanted groups compared with the vehicle-injected group (A). The spared tissue was measured in transversal sections of the injured spinal cord segment immunostained for GFAP. A decrease of the preserved area was observed at 63 days posttransplant (dpt) in the epicenter of the lesion and rostrocaudally in both transplanted groups in comparison with the vehicle group (B, vehicle; C, acute; D, subacute). Quantification of the area of spared tissue, expressed as percentage of the total cross section area, along 1 cm of injured spinal cord in the studied groups, and percentage of spared tissue volume in the same segment (E). $*p<0.05$, $***p<0.001$. At 63 dpt: acute ($n=5$), subacute ($n=6$), and vehicle ($n=6$).

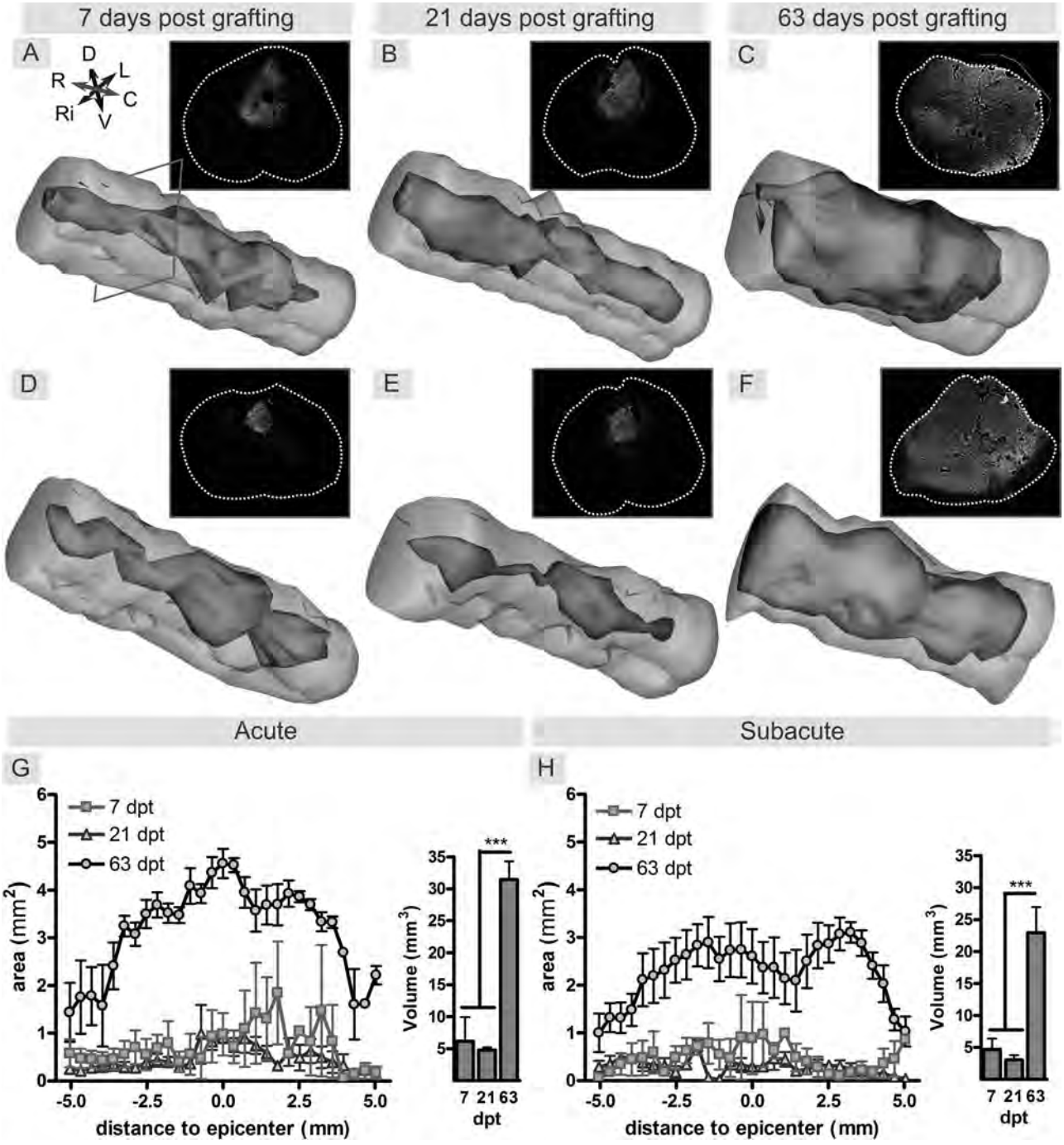

Figure 4. Grafted cell survival and localization in the injured spinal cord. The amount of grafted cells along 1 cm of the injured spinal cord was studied at 7, 21, and 63 dpt by immunolabeling with human marker SC121 (A–F). The grafted cells occupied the main part of the spinal cord at 63 dpt, filling an area that was significantly increased compared to the area at 7 and 21 days (G, H). ***$p<0.001$. Acute and subacute transplanted groups: at 7 dpt ($n=3$), 21 dpt ($n=4$), and 63 dpt ($n=6$).

group: 11±4%; subacute transplant group: 21.58±5%) to 21 dpt (acute transplant group: 21.79±9%; subacute transplant group: 23.97±1%), whereas the expression of GFAP increased significantly from 7 and 21 to 63 dpt (acute transplant group: 38.82±7%; subacute transplant group: 48.46±6%) in both transplanted groups. On the other hand, SC121 and GFAP colocalization in the periphery of the graft increased significantly only from 21 dpt (acute transplant group: 25.01±2%; subacute transplant group: 17.32±4%) to 63 dpt (acute

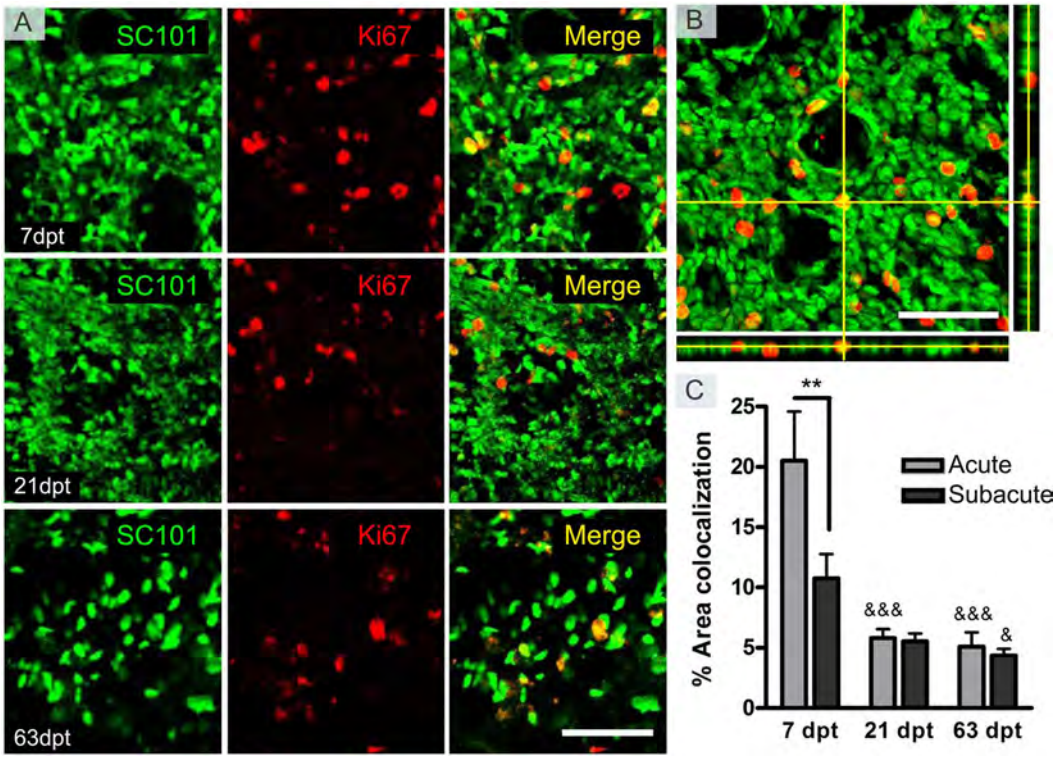

Figure 5. iPSC-derived NSCs still proliferate within the spinal cord at 63 days after transplantation. iPSC-derived NSCs immunostained with the proliferation marker Ki-67 and the human nuclear marker SC101 in transverse sections of the injured spinal cord at 7, 21, and 63 dpt in both transplanted groups (A). The orthogonal view from confocal image shows colocalization between both markers (B). The amount of colocalization between Ki-67 and SC101 was measured as the percentage of the Ki-67 area coincident with the SC101 area. The results indicated significantly higher proliferation at 7 dpt compared to 21 and 63 dpt in both groups (C). The number of SC101-Ki-67-positive cells decreased with time, but at the end of the follow-up, there were still proliferating grafted cells. $^{**}p<0.01$, 0 dpi group versus 7 dpi group; $\&p<0.05$, $\&\&\&p<0.001$, 21 and 63 dpt versus 7 dpt. Scale bar: 50 μm. Acute and subacute transplanted groups: at 7 dpt ($n=3$), 21 dpt ($n=4$), and 63 dpt ($n=6$).

transplant group: 37.30±4%; subacute transplant group: 32.79±4%) (Fig. 7A–D). Differentiation of the iPSC-derived NSCs into astrocytes was observed at earlier time in the graft edge than in the center of the graft. As mentioned above, we did not observe expression of oligodendrocyte markers, CNPase or Ng2, in the grafted iPSC-derived NSCs at any time throughout the study. Moreover, we observed that in both cell-transplanted groups, around 40% of the cells were positive for nestin, suggesting that these cells remained undifferentiated (Fig. 8).

These results indicate that grafted iPSC-derived NSCs were able to survive and proliferate within the injured tissue. Moreover, the cells were able to express neuronal and astroglial phenotypes. Most of the NSCs differentiated into neurons, but only a low proportion were mature neurons, indicating that iPSC-derived NSCs were unable to fully differentiate in the lesion site of SCI rats. The expression of Nestin suggests that almost half of the transplanted cells were at a nondifferentiated stage, which could explain their continued proliferation (Fig. 8).

The SCI Environment Induces iPSC-Derived NSC Proliferation In Vitro

In order to analyze further how the spinal cord microenvironment can affect the iPSC-derived NSC phenotype, the cells were cultured in vitro with the addition of protein lysate from intact or injured spinal cord. It is worth noting

FACING PAGE

Figure 6. Expression of neuronal markers by grafted iPSC-derived NSCs. Confocal image colocalization of the human markers (SC121 and SC101) and the neuronal markers β-III tubulin (A) and NeuN (B) at 7, 21, and 63 dpt in both acute and subacute transplanted groups. β-III tubulin expression increased significantly from 7 and 21 dpt to 63 dpt (C, D). NeuN expression was significantly increased at 63 dpt compared to 7 and 21 dpt (C, D). $^{*}p<0.05$, $^{**}p<0.01$. Scale bar: 100 μm. Acute and subacute transplanted groups: at 7 dpt ($n=3$), 21 dpt ($n=4$), and 63 dpt ($n=6$).

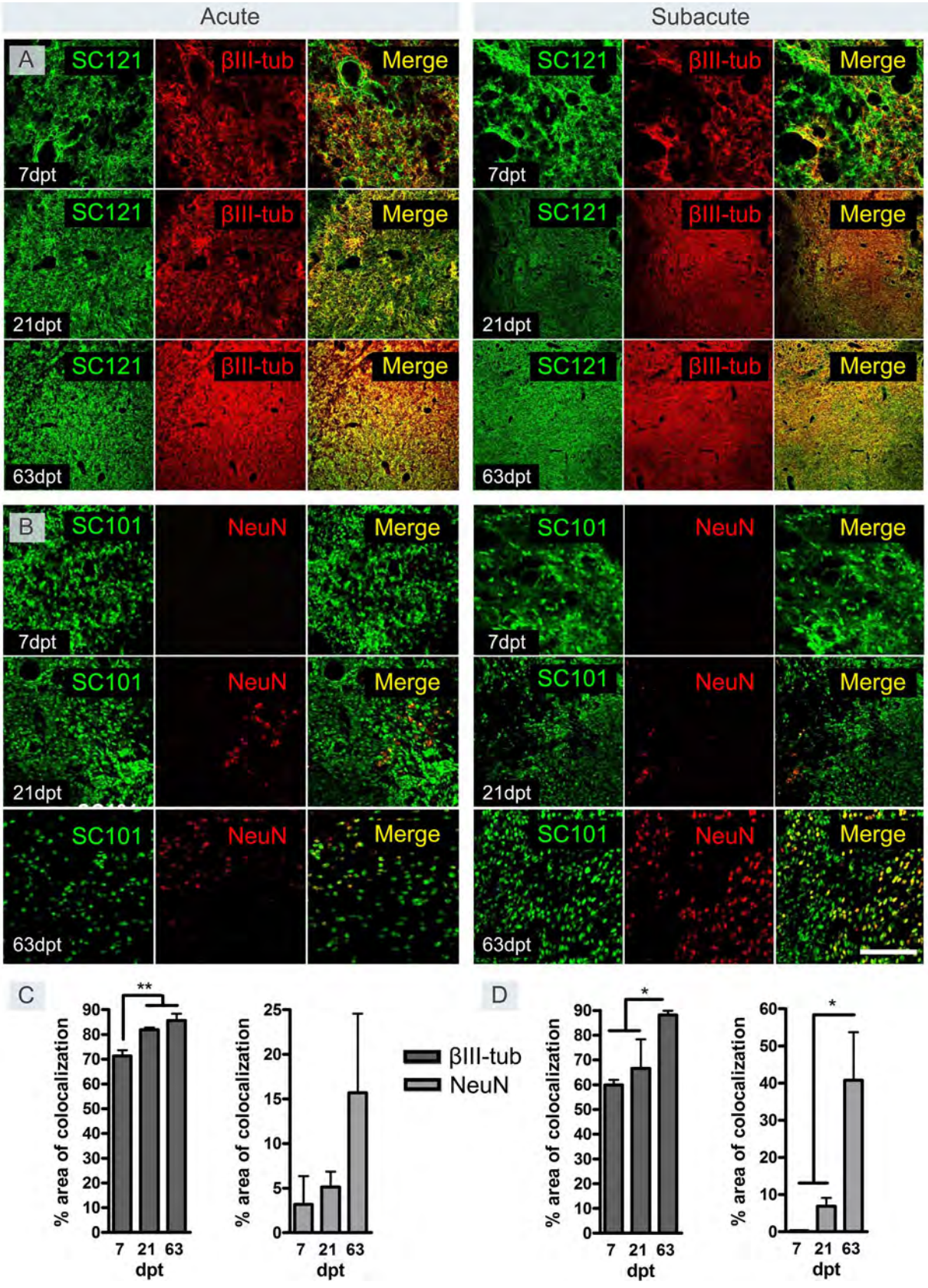
Acute
Subacute
A
SC121
βIII-tub
Merge
7dpt
21dpt
63dpt
B
SC101
NeuN
C
D
% area of colocalization
dpt
βIII-tub
NeuN
**
*

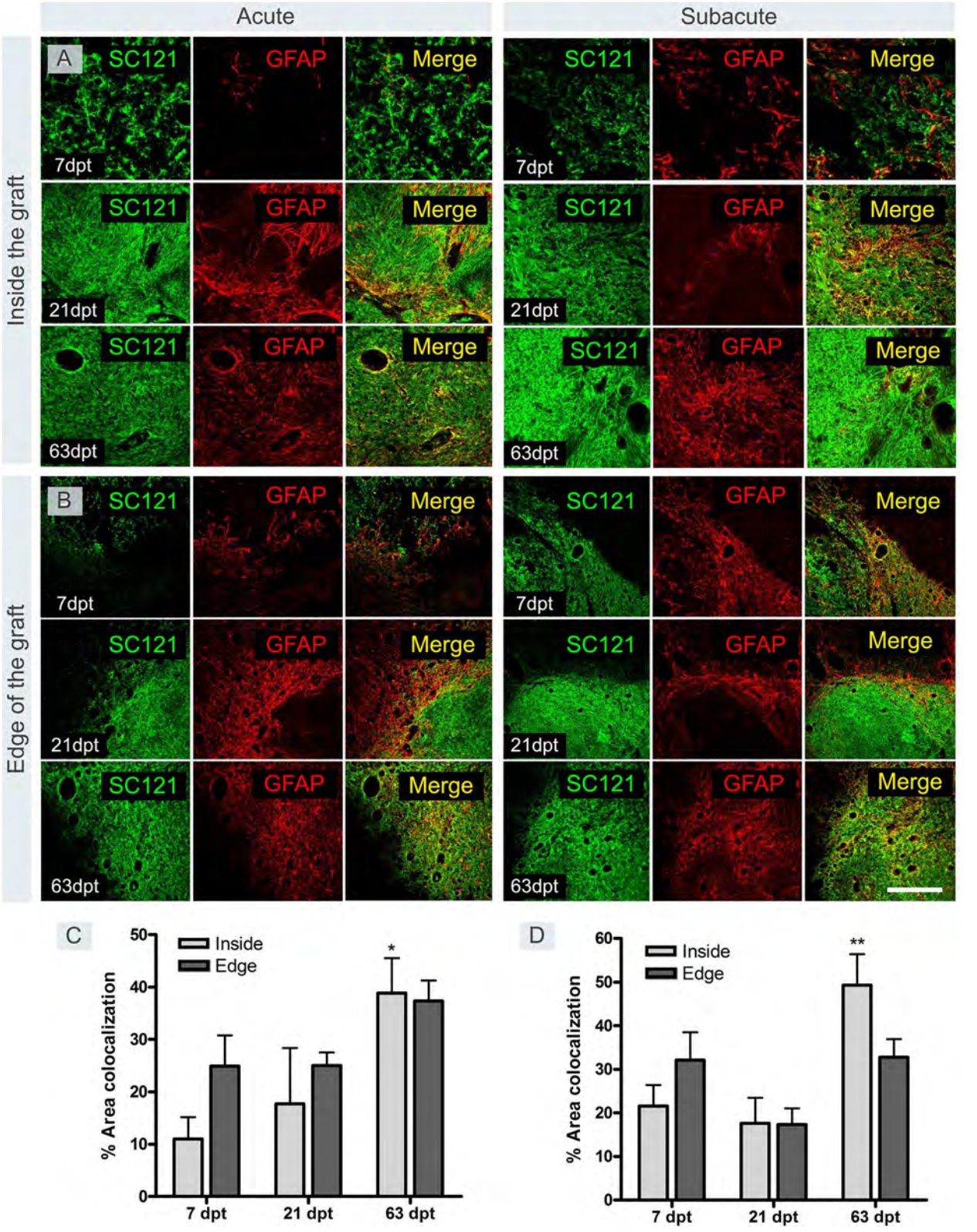

Figure 7. GFAP expression by grafted iPSC-derived NSCs. Colocalization of glial fibrillary acidic protein (GFAP) with human SC121 marker at the middle (A) and at the edge (B) of the graft at 7, 21, and 63 dpt. The expression of GFAP significantly increased from 7 and 21 dpt to 63 dpt in the middle (C, D), and from 21 to 63 dpt in the periphery (C, D). $*p<0.05$, $**p<0.01$. Scale bar: 100 μm. Acute and subacute transplanted groups: at 7 dpt ($n=3$), 21 dpt ($n=4$), and 63 dpt ($n=6$).

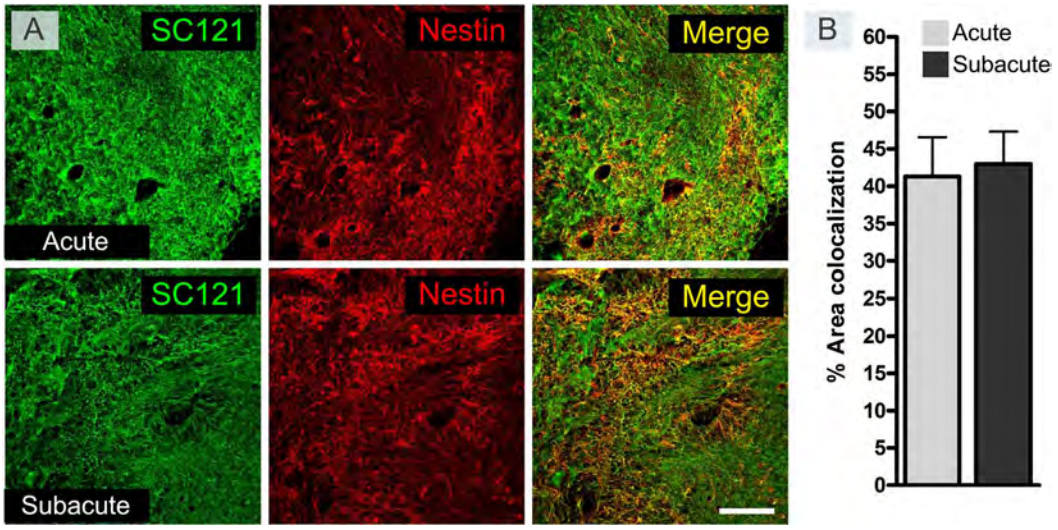

Figure 8. Nestin expression of the grafted iPSC-derived NSCs at the end of the follow-up. The colocalization of the nestin marker with the human SC121 marker was analyzed at 63 dpt in both groups that received the cell transplant acutely (at 0 dpi) or subacutely (at 7 dpi) (A). Around 40% of the SC121-positive iPSC-derived NSC area was also positive for nestin (B). No significant difference was observed between groups. Scale bar: 200 μm. At 63 dpt: acute and subacute transplanted groups ($n=6$).

that during the spinal cord extraction, there is an unavoidable damage to the cord tissue due to ischemia and the dissection process. Therefore, what we here name as "intact" spinal cord lysate is in fact an injury niche by itself, but without a previous lesion. By confocal microscopy we observed that some of the iPSC-derived NSCs were positive for nestin (Fig. 9E–H) and Ki-67 (Fig. 9I–L), indicating that the cells remained nondifferentiated and in a proliferative state for 3 days under the influence of the injured spinal cord lysates. Moreover, β-III tubulin-positive cells were found (Fig. 9A–D), indicating that some of the iPSC-derived NSCs were able to differentiate into nonmature neural lineage cells at 3 days after plating, independently of the type of extract added to the culture. The MTT cell viability assay (Fig. 9M) showed that iPSC-derived NSCs in the presence of lysate from intact, 7- and 14-dpi spinal cords had a significant increase in proliferation, compared to control cultures without extract (Fig. 9I–L). The lysate from previously injured spinal cords had increased MTT activity during the first day in vitro in comparison with lysate from the intact spinal cord. In contrast, lysates from previously injured spinal cords produced significantly less iPSC-derived NSC proliferation than the lysate from intact cords at 2 and 3 days in culture. This could be due to changes in the proliferative capacity of the cells exposed in vitro to injured spinal cord lysate over time or to detrimental factors that provoke major cell death. These results suggest that the injured spinal cord environment contains factors that induce proliferation of iPSC-derived NSCs without changes in their immature stage.

DISCUSSION

The generation of human NSCs from iPSCs may be a promising cell source for autologous transplantation in the treatment of SCI[20]. hiPSC-derived NSCs have been transplanted after SCI in mice, rats, and marmosets, promoting functional recovery in some cases[13]. However, other studies have demonstrated that there are important differences in tumorigenicity and responsiveness to neural induction signals of iPSCs derived from various somatic tissues. For instance, transplanted mouse embryonic iPSC clone-derived NSCs were able to differentiate into neurospheres and showed good survival, differentiation into neurons, astrocytes, and oligodendrocytes, and posttransplantation safety in the lesion site of an SCI mouse model without teratoma formation. On the other hand, transplanted adult mouse tissue (tip tail fibroblasts)-derived iPSCs showed resistance to differentiation, and most of the cells remained in an undifferentiated stage, even after the protocol for inducing differentiation[11]. In this case, teratoma formation was observed. These contradictory findings suggest that iPSCs derived from adult tissue are not as safe as iPSCs derived from embryonic tissue[21]. Unfortunately, the use of human embryos as a source comes with difficulty in generating patient-specific ESCs and ethical controversies that hinder their clinical application. Therefore, research efforts are now focused on the use of iPSCs derived from adult somatic cells to establish a cell source that allows the autologous transplantation of patient-specific cells[22,23]. Nowadays, most reprogramming techniques rely on the factors Oct4, Sox2, Klf4, and c-Myc (referred to as OSKM), and

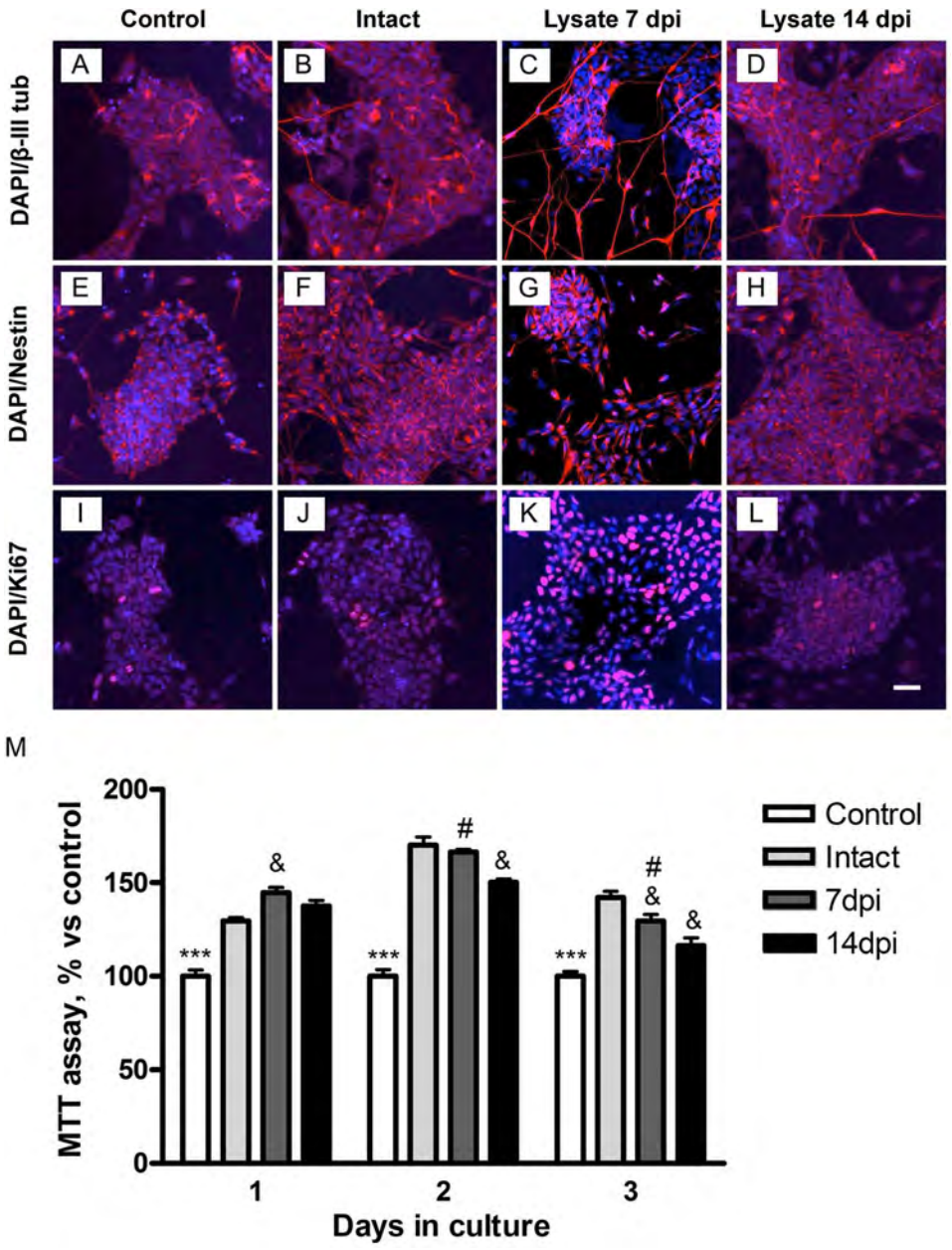

Figure 9. In vitro iPSC-derived NSCs' response after incubation with a lysate of intact and injured spinal cord. Cells were positive for β-III tubulin (A–D), nestin (E–H), and Ki-67 (I–L). The viability test showed an increase of cell proliferation (M) in the presence of the injured cord lysate at 7 dpi. ***$p < 0.001$, control versus addition of lysates; &$p < 0.05$, intact versus 7 and 14 dpi lysates; #$p < 0.05$, 7 dpi versus 14 dpi lysates. Scale bar: 50 μm. Intact ($n = 3$), 7 dpi ($n = 3$), and 14 dpi ($n = 3$).

various methods are used for their delivery into cells, which are divided into viral[21] and nonviral methods[24,25]. However, they entail some risks that could be avoided by using synthetic mRNA transfection of the four factors, removing c-Myc[26]. Another possible source of cells is from direct reprogramming somatic cells, bypassing the pluripotent stages; in vivo conversion of astrocytes into neurons in injured adult spinal cords and further maturation have been shown in mice[27].

In order to analyze how the SCI environment affects the survival and differentiation pattern of adult hiPSC-derived NSCs, we transplanted them into the spinal cord of rats after a contusion injury. It is important to note that vehicle was used as a control instead of nonviable cells. The aim of the transplantation study was to test the effect of the cells, regardless of the vehicle used for transplantation. Nonviable cells could change the spinal cord environment due to specific reactions against them, making it difficult to conclude

if the differences between groups were produced by the vehicle or the presence of cells (alive or not). Our results reveal that the grafted cells grew and expanded inside of the injured spinal cord, filling the cavity but also affecting spared tissue. This was associated with a decrease of functional recovery of the transplanted SCI animals at the late phase. This observation could be related to the number of cells that remained undifferentiated and in a proliferative stage until late time points after transplantation.

Adult hiPSC-Derived NSCs Proliferated Inside the Injured Tissue Compromising Functional Recovery

In the present study, we found that the grafted iPSC-derived NSCs were able to expand through the injury site over time, indicating that the injury niche allows the maintenance of a proliferative state. Similarly, the cord injury niche enhanced iPSC-derived NSC proliferation in vitro, suggesting that the production of soluble factors induces proliferation early after injury. These results are in agreement with the higher amount of Ki-67-positive iPSC-derived NSCs 1 week after grafting in rats transplanted on the same day (0 dpi) than in rats with delayed (7 dpi) transplant. Similar results were reported by Sontag et al., who found that human NSCs propagated as neurospheres proliferated more between 1 and 28 dpt than later, between 28 and 98 dpt, in the injured spinal cord[27]. It is worth noting that while the in vitro experiments showed an increase in cell number without apparent changes in Ki-67 expression, in the in vivo experiments the number of proliferating cells decreased with time. The partial differentiation and maturation of the cells after transplantation may explain the reduction in the amount of proliferative cells. A previous study showed that the expansion pattern of fetal brain tissue-derived hNSCs after transplantation changes depending on the distance from the epicenter of the lesion at long time points[27]. The same study also demonstrated that the transplantation niche and the injured microenvironment have effects on the spatiotemporal dynamics of hNSC engraftment, similar to what we found with our NSCs derived from adult iPSCs. Since we transplanted human NSCs into rat spinal cords, rats were treated with FK506, an immunosuppressive drug that prevents immunological rejection against the grafted cells[28]. Therefore, we cannot dismiss the possibility that the immunosuppression favored the proliferation of the transplanted cells. Nevertheless, with the low dose of FK506 administered, there was still some degree of microglial reaction against the grafted cells (see supplementary Fig. 4; available at: https://www.dropbox.com/sh/aiaq83057uij1c0/AADTehQ_p4b524GALv1H14Zya?dl=0). Other studies in SCI using histocompatible approaches of iPSC-derived NSC transplantation also showed tumorigenic-like activity of the grafted cells[11]. The high proliferation of the iPSC-derived NSCs at short time points and the low but continuous proliferation at longer time points explain the overgrowth of grafted tissue, forming a cell mass inside the injured and transplanted spinal cords. The teratogenic activity of our iPSC-derived NSCs may be a consequence of the reprogramming of adult somatic cells[11,29], which seems not to happen with hNSCs obtained directly from adult spinal cord donors[30].

The expansion of the grafted iPSC-derived NSCs in the injured spinal cord resulted in an enlargement of the volume of damaged tissue with a decrease of spared tissue. The 200-kdyn contusion injury leads to a drastic destruction of the spinal cord parenchyma at the epicenter and extends along several segments, interrupting most motor descending tracts, as demonstrated by the abolition of MEPs and marked locomotor deficits. Interestingly, functional recovery of the transplanted animals was similar or slightly better than that of vehicle-injected rats during the early phase of the follow-up. However, around 4–6 weeks after transplantation, the performance of the animals transplanted with iPSC-derived NSCs showed a progressive decline, reflected by a reduction in the BBB subscore, the running capacity, and the MEP amplitude. At the end of the study, histological analysis showed that the transplanted groups had less residual tissue at ventral and lateral regions of the cord than vehicle-injected animals, thereby explaining the decrease in the locomotor score of engrafted rats with time. The explanation for this late functional reduction in transplanted animals is likely the progressive increase of the cell mass inside the injured cord.

Contrary to our findings, some previous studies with hiPSC-derived NSCs have shown some functional benefits in the transplanted animals. Therefore, it is important to consider the differences between studies. Regarding the source of NSCs, the derivation protocol of neural lineage cells from iPSCs may be crucial to obtain different NSCs. For instance, some studies have used the NSC culture system in neurospheres, which is composed of free-floating clusters of NSCs. The neurosphere passage can determine the fate of the NSCs, since the differentiation of primary neurospheres is mainly into neurons, whereas secondary neurospheres mature into a mixed population of neurons, astrocytes, and oligodendrocytes[8]. Therefore, although Nori et al.[2] and Kobayashi et al.[9] used a similar contusion model to in our study, they transplanted iPSC-derived NSCs from tertiary neurospheres with a later determination period than our adherent cells. This suggests that adult cells are more vulnerable to changes induced by the injured environment than fetal cells, even though a recent study claims that the use of NSCs coming from aged fibroblasts might not be a limiting factor[22]. Furthermore, the use of certain factors during reprogramming may enhance neurite outgrowth, maturation, and expression of different neural markers[31], influencing engraftment and differentiation within the injured nervous system[32].

Another important difference between study designs is the type of SCI lesion used. A recent study has shown that NPCs transplanted after spinal cord contusion into immunocompetent mice exhibited poor cell survival, even when mice were under immunosuppressive therapy. Moreover, the transplant did not promote functional recovery[12]. On the contrary, Romanyuk et al. reported that neural progenitors derived from iPSC are able to survive, engraft, migrate, and differentiate within the damaged rat spinal cord after a balloon-induced compression lesion, inducing also functional recovery of the transplanted animals[13]. Different lesion models may provoke different types of damage in the spinal cord, which will be an important determinant for the engraftment of the cells in the tissue.

The SCI Environment Does Not Induce Full Differentiation of Adult iPSC-Derived NSCs

The main goal for NSC transplantation after CNS injuries is the restitution of neural cells and the connectivity between cells that is destroyed by the SCI lesion. For this purpose, appropriate differentiation and integration of the cells in the host tissue are needed. Before transplantation, our cells exhibited a neural stem/progenitor-like phenotype. However, once transplanted, iPSC-derived NSCs differentiated along the neural lineage, expressing a high percentage of β-III tubulin (~85%) and a lower percentage of NeuN (20–40%) at late time points. This means that most of the grafted cells had an immature neuronal phenotype (β-III tubulin$^+$/NeuN$^-$) at 2 months after grafting. Differentiation into astrocytes was also observed. Although our cells were mostly β-III tubulin positive, it has been shown that certain nestin-positive astrocytes derived from human fetal astrocytes can also express low levels of β-III tubulin[33], but this coexpression with the astroglial marker, GFAP, is mainly observed in early proliferative stages, prior to differentiation[34]. Therefore, the β-III tubulin/nestin-positive cells (before transplant) could be NSCs with progenitor potential to produce astrocytes and neurons or could be a mixture of predestined neurons and astroglial progenitors indistinguishable with the markers we used. Interestingly, temporal and spatial differentiation of iPSC-derived NSCs into astrocytes was observed. The higher number of GFAP-positive cells in the external part than in middle areas of the graft at early time points suggests that the close contact with the lesion induces stronger proliferation of astrocytes. In normal conditions, in the surrounding area of the SCI, there is high astrocyte reactivity, which contributes to formation of the glial scar[35]. The lower differentiation of iPSC-derived NSCs into astrocytes in the middle of the graft could be a consequence of the absence of contact with factors coming from the lesion border and might also explain the differentiation of the transplanted cells into neurons instead of astrocytes in this part of the graft.

The differentiation pattern of the NSCs within the injured tissue seems to be important for determining the effects of the transplanted cells on recovery after SCI. The presence of only a few fully mature and functional neurons at the time of behavioral assessment of the animals is one of the causes of poor functional benefits after transplantation[22]. Moreover, in cases where NSCs and NPCs were directly cultured from an adult human spinal cord, transplanted neurospheres in the rat spinal cord after injury generated neurons, astrocytes, and oligodendrocytes, suggesting specific phenotypic potential related to the donor species[30]. This study also showed absence of Ki-67-positive cells at 1 week posttransplantation, indicating that grafted cells became postmitotic. These results suggest that cells coming from specific organs have more complete differentiation into the neural lineage cells than those coming from iPSCs. Therefore, the cell source as well as the injured environment are crucial for the fate of the transplanted cells[26].

CONCLUSIONS

Taken together, the results obtained suggest that β-III tubulin/nestin-positive iPSC-derived NSCs were able to differentiate into neuronal and astroglial lineages once transplanted, but, despite the high percentage of differentiated cells, there was still a proportion of cells that persisted in a neural stem or progenitor stage. The sustained proliferative state of these cells explains the uncontrolled growth of the cell graft within the injured spinal cord and the decrease in functional recovery of the transplanted animals. Moreover, results from in vitro and in vivo experiments suggest that the niche of transplantation and the injured microenvironment affects the differentiation pattern and spatiotemporal dynamics of the iPSC-derived NSCs[27]. Concerning the source of the NSCs, either from embryonic or from adult cells, we verified that NSCs reprogrammed from adult somatic cells have a potential risk for the formation of a tumor-like mass in the graft. Therefore, new experimental approaches are needed to promote and guide cell differentiation, as well as reduce tumorigenicity once the cells are transplanted within the lesion site[36].

ACKNOWLEDGMENTS: This work was supported by TERCEL and CIBERNED funds from the Instituto de Salud Carlos III of Spain, and FEDER funds from the EC. A.B.A.P. is supported by funds from the Fondo de Investigación Sanitaria of Spain 49623. M.J.E. is supported in part by the Program Ramon y Cajal (No. RYC-2010-06512), FBG project 307900, and project grant BFU2011-26596. We acknowledge the help of Guy Ben Ary, from the Department of Anatomy, Physiology and Human Biology, University of Western Australia, Nedlands, Australia, in the development of the cell cultures, supported by an Australian Arts Council Fellowship. We thank the technical assistance of Jessica Jaramillo, Marta Morell, and Mónica Espejo for all the

in vivo experimental work developed. The authors declare no conflicts of interest.

REFERENCES

1. Fujimoto Y, Abematsu M, Falk A, Tsujimura K, Sanosaka T, Juliandi B, Semi K, Namihira M, Komiya S, Smith A, Nakashima K. Treatment of a mouse model of spinal cord injury by transplantation of human induced pluripotent stem cell-derived long-term self-renewing neuroepithelial-like stem cells. Stem Cells 2012;30:1163–73.
2. Nori S, Okada Y, Yasuda A, Tsuji O, Takahashi Y, Kobayashi Y, Fujiyoshi K, Koike M, Uchiyama Y, Ikeda E, Toyama Y, Yamanaka S, Nakamura M, Okano H. Grafted human-induced pluripotent stem-cell-derived neurospheres promote motor functional recovery after spinal cord injury in mice. Proc Natl Acad Sci USA 2011;108:16825–30.
3. Lu P, Jones LL, Snyder EY, Tuszynski MH. Neural stem cells constitutively secrete neurotrophic factors and promote extensive host axonal growth after spinal cord injury. Exp Neurol. 2003;181:115–29.
4. Yan J, Welsh AM, Boka SH, Snyder EY, Koliatsos VE. Differentiation and tropic/trophic effects of exogenous neural precursors in the adult spinal cord. J Comp Neurol. 2004;480:101–14.
5. Pfeifer K, Vroemen M, Blesch A, Weidner N. Adult neural progenitor cells provide a permissive guiding substrate for corticospinal axon growth following spinal cord injury. Eur J Neurosci. 2004;20:1695–704.
6. Karimi-Abdolrezaee S, Eftekharpour E, Wang J, Morshead CM, Fehlings MG. Delayed transplantation of adult neural precursor cells promotes remyelination and functional neurological recovery after spinal cord injury. J Neurosci. 2006;26:3377–89.
7. Dulin JN, Lu P. Bridging the injured spinal cord with neural stem cells. Neural Regen Res. 2014;9:229–31.
8. Okano H. Neural stem cells and strategies for the regeneration of the central nervous system. Proc Jpn Acad Ser B Phys Biol Sci. 2010;86:438–50.
9. Kobayashi Y, Okada Y, Itakura G, Iwai H, Nishimura S, Yasuda A, Nori S, Hikishima K, Konomi T, Fujiyoshi K, Tsuji O, Toyama Y, Yamanaka S, Nakamura M, Okano H. Pre-evaluated safe human iPSC-derived neural stem cells promote functional recovery after spinal cord injury in common marmoset without tumorigenicity. PLoS One 2012;7:e52787.
10. Nutt SE, Chang E-A, Suhr ST, Schlosser LO, Mondello SE, Moritz CT, Cibelli JB, Horner PJ. Caudalized human iPSC-derived neural progenitor cells produce neurons and glia but fail to restore function in an early chronic spinal cord injury model. Exp Neurol. 2013;248:491–503.
11. Tsuji O, Miura K, Fujiyoshi K, Momoshima S, Nakamura M, Okano H. Cell therapy for spinal cord injury by neural stem/progenitor cells derived from iPS/ES cells. Neurotherapeutics 2011;8:668–76.
12. Pomeshchik Y, Puttonen KA, Kidin I, Ruponen M, Lehtonen S, Malm T, Åkesson E, Hovatta O, Koistinaho J. Transplanted human induced pluripotent stem cell-derived neural progenitor cells do not promote functional recovery of pharmacologically immunosuppressed mice with contusion spinal cord injury. Cell Transplant. 2015;24:1799–812.
13. Romanyuk N, Amemori T, Turnovcova K, Prochazka P, Onteniente B, Sykova E, Jendelova P. Beneficial effect of human induced pluripotent stem cell-derived neural precursors in spinal cord injury repair. Cell Transplant. 2015;24:1781–97.
14. Ruggieri M, Riboldi G, Brajkovic S, Bucchia M, Bresolin N, Comi GP, Corti S. Induced neural stem cells: Methods of reprogramming and potential therapeutic applications. Prog Neurobiol. 2014;114:15–24.
15. Gonzalez F, Barragan-Monasterio M, Tiscornia G, Montserrat-Pulido N, Vassena R, Batlle-Morera L, Rodriguez-Piza I, Izpisua-Belmonte JC. Generation of mouse-induced pluripotent stem cells by transient expression of a single non-viral polycistronic vector. Proc Natl Acad Sci USA 2009; 106:8918–22.
16. Basso DM, Beattie MS, Bresnahan JC. A sensitive and reliable locomotor rating scale for open field testing in rats. J Neurotrauma 1995;12:1–20.
17. Basso DM. Behavioral testing after spinal cord injury: Congruities, complexities, and controversies. J Neurotrauma 2004;21:395–404.
18. Rosen GD, Harry JD. Brain volume estimation from serial section measurements: A comparison of methodologies. J Neurosci Methods 1990;35:115–24.
19. Fiala JC. Reconstruct: A free editor for serial section microscopy. J Microsc. 2005;218:52–61.
20. Hodgetts SI, Stagg K, Sturm M, Edel M, Blancafort P. Long live the stem cell: The use of stem cells isolated from post mortem tissues for translational strategies. Int J Biochem Cell Biol. 2014;56:74–81.
21. Takahashi K, Tanabe K, Ohnuki M, Narita M, Ichisaka T, Tomoda K, Yamanaka S. Induction of pluripotent stem cells from adult human fibroblasts by defined factors. Cell 2007;131:861–72.
22. Lu P, Lee-Kubli C. Induced pluripotent stem cell-derived neural stem cell therapies for spinal cord injury. Neural Regen Res. 2015;10:10.
23. Su Z, Niu W, Liu ML, Zou Y, Zhang CL. In vivo conversion of astrocytes to neurons in the injured adult spinal cord. Nat Comm. 2014;5:3338.
24. Fusaki N, Ban H, Nishiyama A, Saeki K, Hasegawa M. Efficient induction of transgene-free human pluripotent stem cells using a vector based on Sendai virus, an RNA virus that does not integrate into the host genome. Proc Jpn Acad Ser B Phys Biol Sci. 2009;85:348–62.
25. Warren L, Manos PD, Ahfeldt T, Loh YH, Li H, Lau F, Ebina W, Mandal PK, Smith ZD, Meissner A, Daley GQ, Brack AS, Collins JJ, Cowan C, Schlaeger TM, Rossi DJ. Highly efficient reprogramming to pluripotency and directed differentiation of human cells with synthetic modified mRNA. Cell Stem Cell 2010;7:618–30.
26. Alvarez-Palomo AB, McLenachan S, Chen FK, Da Cruz L, Dilley RJ, Requena J, Lucas M, Lucas A, Drukker M, Edel MJ. Prospects for clinical use of reprogrammed cells for autologous treatment of macular degeneration. Fibrogenesis Tissue Repair 2015;8:9.
27. Sontag CJ, Uchida N, Cummings BJ, Anderson AJ. Injury to the spinal cord niche alters the engraftment dynamics of human neural stem cells. Stem Cell Reports 2014;2:620–32.
28. Torres-Espín A, Redondo-Castro E, Hernández J, Navarro X. Bone marrow mesenchymal stromal cells and olfactory ensheathing cells transplantation after spinal cord injury-a morphological and functional comparison in rats. Eur J Neurosci. 2014;39:1704–17.
29. Miura K, Okada Y, Aoi T, Okada A, Takahashi K, Okita K, Nakagawa M, Koyanagi M, Tanabe K, Ohnuki M, Ogawa

D, Ikeda E, Okano H, Yamanaka S. Variation in the safety of induced pluripotent stem cell lines. Nat Biotechnol. 2009;27:743–5.
30. Mothe AJ, Zahir T, Santaguida C, Cook D, Tator CH. Neural stem/progenitor cells from the adult human spinal cord are multipotent and self-renewing and differentiate after transplantation. PLoS One 2011;6:e27079.
31. Hsu YC, Chen SL. Wang YJ, Chen YH, Wang DY, Chen L, Chen CH, Chen HH, Chiu IM. Signaling adaptator protein SH2B1 enhances neurite outgrowth and accelerates the maturation of human induced neurons. Stem Cells Transl Med. 2014;3:713–22.
32. Wakeman D, Redmond DE, Dodiya HB, Sladek JR, Leranth C, Teng YD, Samulski RJ, Snyder EY. Human neural stem cells survive long term in the midbrain of dopamine-depleted monkeys after GDNF overexpression and project neurites toward an appropriate target. Stem Cells Transl Med. 2014;3:692–701.
33. Dráberová E, Valle L, Gordon J, Chadarevian JP, Agamanolis D, Legido A, Khalili KD. Class III beta-tubulin is constitutively coexpressed with glial fibrillary acidic protein and nestin in midgestational human fetal astrocytes: Implications for phenotypic identity. J Neuropathol Exp Neurol. 2008;67:341–54.
34. Rieske P, Azizi SA, Augelli B, Gaughan J, Krynska B. A population of human brain parenchymal cells express markers of glial, neuronal and early neural cells and differentiate into cells of neuronal and glial lineages. Eur J Neurosci. 2007;25:31–7.
35. Silver J, Miller JH. Regeneration beyond the glial scar. Nat Rev Neurosci. 2004;5:146–56.
36. Wyles SP, Yamada S, Oommen S, Maleszewski JJ, Beraldi R, Martinez-Fernandez A, Terzic A, Nelson TJ. Inhibition of DNA topoisomerase II selectively reduces the threat of tumorigenicity following induced pluripotent stem cell-based myocardial therapy. Stem Cells Dev. 2014;23:1–9.